SCIENCE TRANSLATIONAL MEDICINE | RESEARCH ARTICLE

BONE

BMPR1A maintains skeletal stem cell properties in craniofacial development and craniosynostosis

Takamitsu Maruyama[1,2], Ronay Stevens[1], Alan Boka[1], Laura DiRienzo[1], Connie Chang[1], Hsiao-Man Ivy Yu[1], Katsuhiko Nishimori[3], Clinton Morrison[4], Wei Hsu[1,5,6]*

Skeletal stem cells from the suture mesenchyme, which are referred to as suture stem cells (SuSCs), exhibit long-term self-renewal, clonal expansion, and multipotency. These SuSCs reside in the suture midline and serve as the skeletal stem cell population responsible for calvarial development, homeostasis, injury repair, and regeneration. The ability of SuSCs to engraft in injury site to replace the damaged skeleton supports their potential use for stem cell–based therapy. Here, we identified BMPR1A as essential for SuSC self-renewal and SuSC-mediated bone formation. SuSC-specific disruption of *Bmpr1a* in mice caused precocious differentiation, leading to craniosynostosis initiated at the suture midline, which is the stem cell niche. We found that BMPR1A is a cell surface marker of human SuSCs. Using an ex vivo system, we showed that SuSCs maintained stemness properties for an extended period without losing the osteogenic ability. This study advances our knowledge base of congenital deformity and regenerative medicine mediated by skeletal stem cells.

INTRODUCTION

Large craniofacial bone defects, which are caused by various conditions, including trauma, infection, tumors, congenital disorders, and progressive deforming diseases, are major health issues (*1*). The autologous bone graft is a recommended procedure for extensive skeletal repairs, but their success remains highly challenging owing to several limitations (*1*, *2*). Consequently, alternative approaches have been explored (*3*, *4*). Stem cell–based therapy is particularly attractive and promising, in light of the characterization of skeletal stem cells in craniofacial and body skeletons (*5*–*11*). Craniofacial bone is mainly formed through intramembranous ossification, a process different from the endochondral ossification required for the body skeleton (*12*). Because of the distinct properties of the stem cells of the craniofacial and body skeletons (*5*, *13*), it is necessary to study each type of skeletal stem cells. Suture stem cells (SuSCs) are the stem cell population that is naturally programmed to form intramembranous bones during craniofacial skeletogenesis (*5*). Presently, the lack of a cell surface marker for stem cell isolation and the inability to maintain stemness characteristics ex vivo are two critical hurdles that restrict further advances in the field of skeletal regeneration.

Craniosynostosis, which affects 1 in ~2500 individuals, is one of the most common congenital deformities and is caused by premature suture closure (*14*). The suture serving as the growth center for calvarial morphogenesis is the equivalent of the growth plate in the long bone. Excessive intramembranous ossification caused by genetic mutation promotes suture fusion (*15*). An example is the genetic loss of function of AXIN2, which causes craniosynostosis in mice and humans (*16*, *17*). In 2010, we found that craniosynostosis can also be caused by mesenchymal cell fate switching, leading to suture closure through endochondral ossification (*18*). By regulating the interplay between bone morphogenetic protein (BMP) and fibroblast growth factor (FGF) pathways, Axin2-mediated Wnt signaling determines skeletogenic commitment into an osteogenic or chondrogenic lineage. The multipotency further supports the existence of skeletal stem cells within the suture mesenchyme (*18*). Because *Axin2* expression in the presumptive niche site was tightly linked to suture patency, we identified *Axin2*-expressing SuSCs as essential for calvarial development, homeostasis, and injury-induced repair (*5*). The Axin2-positive ($Axin2^+$) SuSCs qualified for the modern, rigorous stem cell definition: They exhibit not only long-term self-renewal, clonal expansion, differentiation, and multipotency but also the ability to repair skeletal defects by direct engraftment and replacement of damaged tissue. However, the mechanism underlying the regulation of SuSC properties and the causal link between SuSC dysregulation and congenital birth defects remain elusive.

RESULTS

Identification of a BMP pathway in Axin2-expressing SuSCs

To identify and isolate $Axin2^+$ cells in the suture mesenchyme and to track the descendants of these cells, we genetically engineered mice that inducibly express a green fluorescent protein (GFP) to reflect the activity from the *Axin2* promoter in a spatiotemporal-specific manner ($Axin2^{GFP}$) (fig. S1A). Using a similar system of inducible expression of Cre to drive either lacZ for β-galactosidase (β-gal) labeling or the fluorescent protein Tomato, we established mouse models permitting the tracing of $Axin2^+$ cells (fig. S1B). From $Axin2^{GFP}$ mice at postnatal day 28 (P28), we isolated the $Axin2^+$ cell population with high-intensity GFP signal ($Axin2^+/GFP^{hi}$) (fig. S1C) and the nonexpressing cell population that is negative for GFP ($Axin2^-/GFP^-$) from the suture mesenchyme.

Microarray analysis comparing SuSCs ($Axin2^+$) and non-SuSCs ($Axin2^-$) revealed about 9000 genes with significant differences ($P < 0.05$, $n = 3$). With pathway analysis using Ingenuity Pathway Analysis (IPA) software, we obtained two scores: an enrichment score, representing the statistically significant accumulation of genes in each pathway,

[1]Center for Oral Biology, University of Rochester Medical Center, Rochester, NY 14642, USA. [2]Department of Dentistry, University of Rochester Medical Center, Rochester, NY 14642, USA. [3]Department of Bioregulation and Pharmacological Medicine and Department of Obesity and Internal Inflammation, Fukushima Medical University, Fukushima City 960-1295, Japan. [4]Department of Surgery, University of Rochester Medical Center, Rochester, NY 14642, USA. [5]Department of Biomedical Genetics, University of Rochester Medical Center, Rochester, NY 14642, USA. [6]Stem Cell and Regenerative Medicine Institute, University of Rochester Medical Center, Rochester, NY 14642, USA.
*Corresponding author. Email: wei_hsu@urmc.rochester.edu, wei_hsu@icloud.com

and a *z* score, representing the activation state of the signal by matching observed and predicted patterns of up-regulation and down-regulation (*19*). In SuSCs, most of the identified signaling pathways were inactive, but the BMP pathway exhibited significant activation (fig. S2A; $P < 10^{-13}$, *z* score > 2.3). Detailed analysis of expression of genes encoding BMP signaling components showed that seven BMP ligands and the type I receptor *Bmpr1a* are up-regulated and two negative regulators (*Smad7* and *Smurf1*) are down-regulated in SuSCs (fig. S2B). The results suggested that BMP ligands signal through Bmpr1a to activate the pathway in SuSCs. Therefore, we examined SuSCs for Bmpr1a in the Axin2$^{Cre\text{-}Dox}$; R26RlacZ model in which SuSCs are marked by lacZ (fig. S1B). Double labeling identified Bmpr1a in Axin2^{+} SuSCs at P28 (fig. S2, C to E), consistent with a role for BMP Bmpr1a signaling in SuSC regulation.

Identification of a requirement of Bmpr1a for SuSC-mediated calvarial development and homeostasis

To delineate the functional importance of BMP signaling in SuSCs, we studied the type I receptors in calvarial morphogenesis (*20*, *21*). Most BMP family members signal through one of three type I receptors—Bmpr1a, Bmpr1b, and Acvr1 (*20*, *21*). We focused on the receptors because there are many BMP ligands, making genetic studies challenging. Mice with global inactivation of *Bmpr1b* are viable, whereas the null mutation of *Bmpr1a* or *Acvr1* is associated with embryonic lethality due to defective mesodermal formation (*22*–*25*). Therefore, we developed Bmpr1a^{Ax2} (Axin2$^{Cre\text{-}Dox}$; Bmpr1a$^{Fx/Fx}$) and Acvr1^{Ax2} (Axin2$^{Cre\text{-}Dox}$; Acvr1$^{Fx/Fx}$) models, enabling doxycycline (Dox)–inducible deletion of *Bmpr1a* or *Acvr1* in the Axin2^{+} SuSCs. For studying the calvarial formation, Dox was administered from embryonic day 16.5 (E16.5) to P3 to initiate Cre-dependent gene deletion (Fig. 1A). The efficiency of Cre-mediated recombination in Axin2^{+} SuSCs and their descendent cells was demonstrated using an R26RlacZ reporter strain (fig. S3, A and B). Immunostaining showed not only the efficacy of *Bmpr1a* ablation in the mutant but also the specificity of the Bmpr1a antibody (fig. S3, C and D).

Bmpr1a^{Ax2}, but not Bmpr1b$^{-/-}$ or Acvr1^{Ax2}, mice displayed craniofacial anomalies at 2 months (Fig. 1B and fig. S4, A and B). The Bmpr1a^{Ax2} mutants were easy to identify by the abnormal skull shape. Micro–computed tomography (μCT) analysis and histology revealed calvarial bone and suture closure abnormalities that were specifically caused by the loss of *Bmpr1a* (Fig. 1, C and D, and fig. S4). The Bmpr1a^{Ax2} skull was significantly shorter without any significant difference in width throughout the first 14 days of postnatal development (fig. S4, A to D; $P < 0.05$). Consequently, the skulls of the Bmpr1a^{Ax2} mutant mice were dome shaped compared to the flatter shape of the skulls of the control mice (fig. S4, E and F). Analysis of skulls stained with alizarin red (fig. S5, A and B), histological analysis (fig. S5, C to H), and μCT analyses (fig. S6) revealed multiple synostoses in the internasal, anterior frontal, sagittal, lambdoid, and squamosal sutures of Bmpr1a^{Ax2} mice. The results indicated a specific requirement of *Bmpr1a* in SuSCs during calvarial morphogenesis.

We previously demonstrated that Axin2^{+} cells function as skeletal stem cells in calvarial development and homeostasis (*5*). To test whether Bmpr1a regulates adult SuSCs, we induced its deletion in the mature skull. In humans, the growth of the skull reaches 90% of adult size in the first year and 95% of adult size by 6 years of age (*26*). The skull size in teenagers is identical to that of adults. In mice,

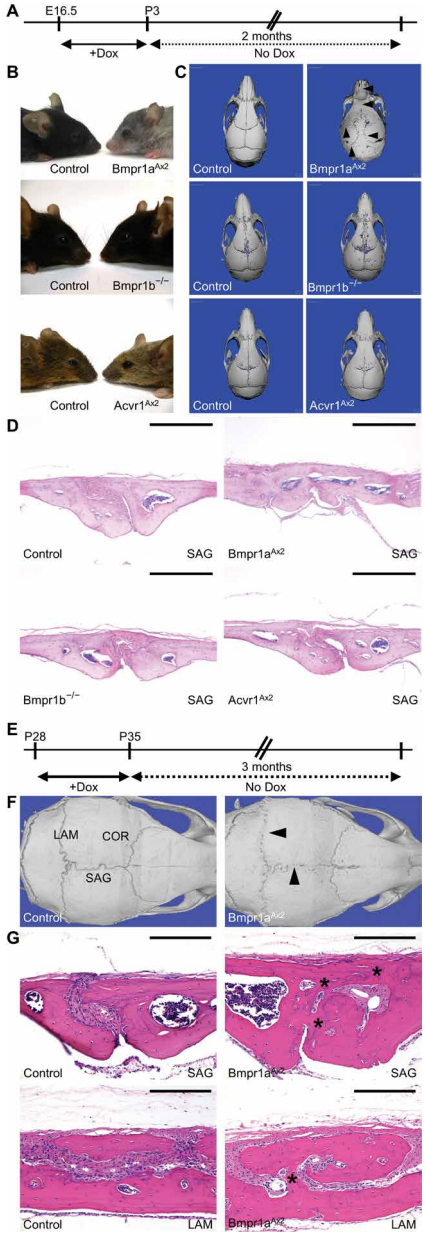

Fig. 1. Stem cell–mediated calvarial development and homeostasis require Bmpr1a. Bmpr1a^{Ax2}, Bmpr1a$^{-/-}$, and Acvr1^{Ax2} mouse models examine BMP type I receptors in calvarial morphogenesis. (**A**) Diagram illustrates the procedure for inducing *Bmpr1a* or *Acvr1* deletion during calvarial development in Axin2^{+} SuSCs using Axin2$^{Cre\text{-}Dox}$ (Axin2-rtTA; TRE-Cre) mice. Control mice were Axin2-rtTA; Bmpr1a$^{Fx/Fx}$ or TRE-Cre; Bmpr1a$^{Fx/Fx}$ mice with Dox for Bmpr1a^{Ax2} mice, Bmpr1b$^{+/-}$ mice for Bmpr1b$^{-/-}$ mice, and Axin2-rtTA; Acvr1$^{Fx/Fx}$ or TRE-Cre; Acvr1$^{Fx/Fx}$ mice with Dox for Acvr1^{Ax2} mice. Mice were examined at 2 months old ($n = 3$ mice per group). (**B**) Photographs of mouse heads and faces. (**C**) μCT images of skulls of the indicated mice. Arrowheads indicate aberrant suture closure. (**D**) Hematoxylin and eosin staining of calvarial tissue at the sagittal suture. Scale bars, 400 μm. (**E**) Diagram illustrates the deletion of *Bmpr1a* in SuSCs in mice after calvarial development. Control mice were Axin2-rtTA; Bmpr1a$^{Fx/Fx}$ or TRE-Cre; Bmpr1a$^{Fx/Fx}$ mice with Dox. Mice were examined after 3 months ($n = 3$ mice per group). (**F**) μCT images of skulls of the indicated mice. Arrowheads indicate aberrant suture closure. (**G**) Hematoxylin and eosin staining of calvarial tissue at the sagittal and lambdoid sutures. Asterisks indicate aberrant suture closure. Scale bars, 200 μm. COR, coronal suture; LAM, lambdoid suture; SAG, sagittal suture.

90% of the skull development is completed at P28 where SuSCs are restricted to the suture midline (*5*, *27*). Therefore, we administrated Dox to the P28 Bmpr1a^{Ax2} mice for 7 days (Fig. 1E). Three months after the Dox treatment, the mutants were examined by μCT and histology. Deletion of *Bmpr1a* in adult SuSCs resulted in aberrant suture morphogenesis and multiple sutural synostoses (Fig. 1, F and G), suggesting an essential role of Bmpr1a in SuSC-mediated calvarial homeostasis. Thus, together, the analysis of mice lacking *Bmpr1a* during embryonic and early postnatal development along with those lacking *Bmpr1a* after skull maturation indicated that Bmpr1a was critical for both calvarial development and homeostasis.

Craniosynostosis is initiated in the midline of the Bmpr1a^{Ax2} suture

A time-course study was performed to decipher the suture closure process. Dox-inducible deletion of *Bmpr1a* was conducted from E16.5 to P3. Skulls from mice were evaluated by alizarin red staining (Fig. 2A) and Goldner's trichrome staining (Fig. 2B) at P0, P7, and P14 (Fig. 2). At P0, *Bmpr1a* deletion caused a wider suture. However, abnormal ossification within the suture mesenchyme was evident at P7 and P14 in the absence of *Bmpr1a*, ultimately leading to suture closure at 2 months (Fig. 1, C and D). This finding suggested that aberrant ossification is initiated in the suture midline and moves toward the osteogenic fronts.

Calvarial bones are formed through osteoblast-mediated intramembranous ossification. To delineate the aberrant ossification process caused by the SuSC-specific deletion of *Bmpr1a*, we examined osteoblast proliferation and differentiation. In the suture of control mice at P3, immunostaining of Ki67, a marker for cells undergoing mitosis, revealed that most cells are quiescent in the suture mesenchyme but actively proliferating at the osteogenic fronts (Fig. 3A), which is the site where intramembranous ossification occurs toward the suture midline. In the Bmpr1a^{Ax2} mice, the number of Ki67^{+} cells was aberrantly increased in the suture mesenchyme (Fig. 3B). To examine osteoprogenitor cells, we immunostained for Osterix (Osx); to detect osteoblast cells, we performed in situ hybridization of type I collagen (Col1). At P0, Osx^{+} osteoprogenitors were detected only at the osteogenic fronts of both control and Bmpr1a^{Ax2} mice (Fig. 3C). However, at P3, we detected increased numbers of Osx^{+} osteoprogenitors in the suture mesenchyme in response to *Bmpr1a* deletion in SuSCs (Fig. 3C). Rather than clusters of Col1^{+} osteoblasts at the osteogenic fronts were observed in control mouse calvaria; Col1^{+} osteoblasts were found throughout the suture mesenchyme of Bmpr1a^{Ax2} calvaria (Fig. 3D). Compared with sutures of Axin2$^{-/-}$; Fgfr1$^{+/-}$ mice, no type II collagen (Col2)–positive chondrocytes were detected in the mutant (fig. S7), suggesting that the loss of Bmpr1a function does not promote stem cell fate change and the aberrant suture closure was not caused by ectopic chondrogenesis and endochondral ossification. Our findings indicated that aberrant ossification is initiated in the suture mesenchyme rather than the osteogenic fronts.

Signaling effects of Bmpr1a on SuSCs in the developing suture

To examine the downstream pathways affected by the loss of *Bmpr1a* function in SuSCs, we analyzed "canonical" BMP signaling mediated by Smad proteins (*28*) and "noncanonical" signaling through kinases (*29*). BMPs that signal through Bmpr1a activate the transcriptional regulators Smad1, Smad5, or Smad8, or some combination thereof (collectively, Smad1/5/8). Immunostaining showed comparable amounts of phosphorylated Smad1/5/8 in the osteogenic front and periosteum of control and Bmpr1a^{Ax2} (fig. S8A, top). However, the amount of phosphorylated Smad1/5/8 appeared less in the Bmpr1a^{Ax2} suture midline (fig. S8A, bottom). Immunostaining of phosphorylated TAK1 indicated activation of this kinase mainly in the osteogenic front, and similar amounts of phosphorylated TAK1 were present in the osteogenic front and suture region of control and Bmpr1a^{Ax2} mice (fig. S8B). Examination of activation of mitogen-activated protein kinases (MAPKs) downstream of Tak1 showed strong activation (phosphorylation) of p38 but not of c-Jun

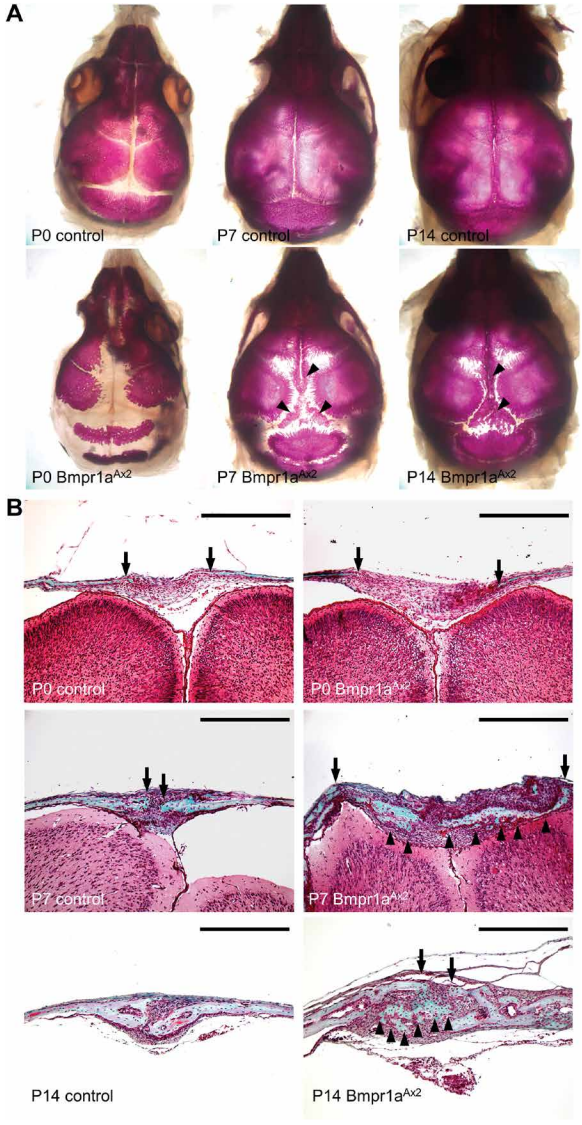

Fig. 2. Craniosynostosis caused by SuSC-specific disruption of *Bmpr1a* involves an unusual suture closure process. Bmpr1a^{Ax2} mice were induced with Dox from E16.5 to P3. Control mice were Axin2-rtTA; Bmpr1a$^{Fx/Fx}$ or TRE-Cre; Bmpr1a$^{Fx/Fx}$ mice with Dox. Skulls of mice of the indicated conditions were analyzed at P0, P7, or P14 ($n = 3$ mice per group). (**A**) Alizarin red staining of intact skulls. (**B**) Goldner's trichome staining of calvarial sections along sagittal suture. Arrowheads indicate mineralization between calvarial bone plates. Arrows indicate osteogenic fronts. Scale bar, 400 μm.

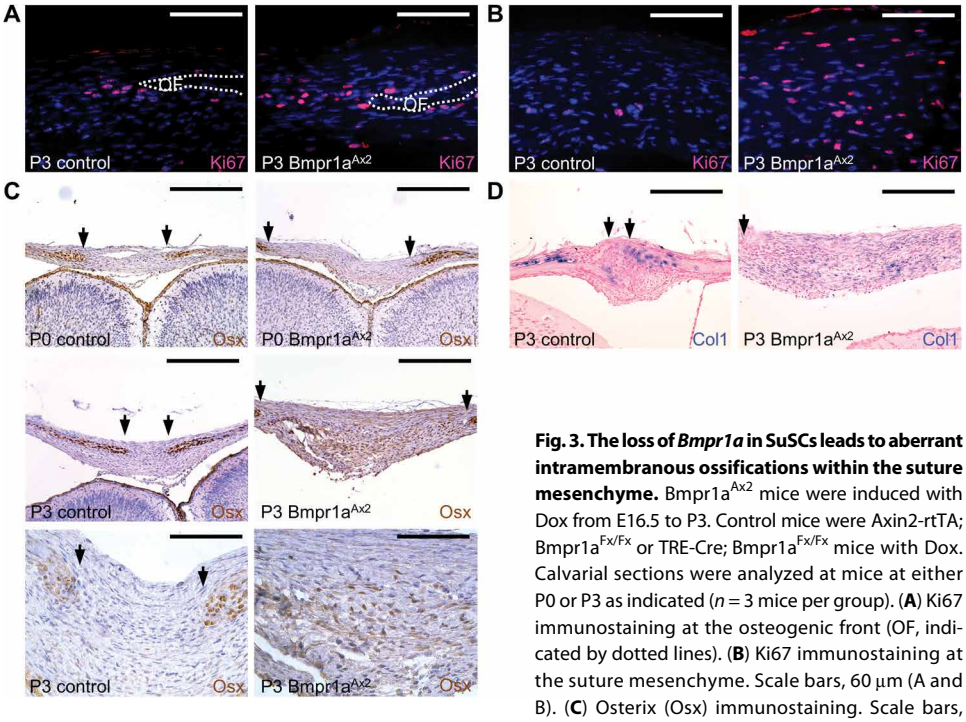

Fig. 3. The loss of *Bmpr1a* in SuSCs leads to aberrant intramembranous ossifications within the suture mesenchyme. Bmpr1a^{Ax2} mice were induced with Dox from E16.5 to P3. Control mice were Axin2-rtTA; Bmpr1a$^{Fx/Fx}$ or TRE-Cre; Bmpr1a$^{Fx/Fx}$ mice with Dox. Calvarial sections were analyzed at mice at either P0 or P3 as indicated ($n = 3$ mice per group). (**A**) Ki67 immunostaining at the osteogenic front (OF, indicated by dotted lines). (**B**) Ki67 immunostaining at the suture mesenchyme. Scale bars, 60 μm (A and B). (**C**) Osterix (Osx) immunostaining. Scale bars, 400 μm (upper four images) and 100 μm (lower two images). (**D**) In situ hybridization of type I collagen (Col1). Scale bars, 200 μm. In (C) and (D), arrows indicate osteogenic fronts.

N-terminal kinase (JNK) (fig. S8C). The other MAPK extracellular signal–regulated kinase (Erk) was also abundant in the mutant (fig. S8C). These results indicated that deletion of *Bmpr1a* reduced canonical but enhanced noncanonical signaling in SuSCs, leading to precocious differentiation in the suture midline and craniosynostosis.

Bmpr1a is required for maintenance of SuSCs

The enhanced cell proliferation and numbers of osteoprogenitors and osteoblasts in the Bmpr1a^{Ax2} suture mesenchyme (Fig. 3) implied a potential role of Bmpr1a in stem cell maintenance. We hypothesized that the loss of *Bmpr1a* depletes the stem cell population leading to precocious osteoblast differentiation and intramembranous ossification. To test our hypothesis, we examined SuSC characteristics of Bmpr1a^{Ax2}. By in vivo clonal expansion analysis, we showed the ability of a single Axin2$^+$ SuSC to generate calvarial bone upon implantation into the kidney capsule (*5*). With limiting dilution analysis, we further established a quantitative method to examine stem cell clonal expansion in the transplanted kidney to measure stem cell frequency (*5*). We used this assay to investigate whether Bmpr1a deficiency affects the clonal expansion and number of SuSCs. Various amounts of cells isolated from the control and Bmpr1a^{Ax2} sutures from P5 mice were implanted into the kidney capsule, and then the implanted site was evaluated by von Kossa staining to detect mineralized ectopic bones (Fig. 4A) and by histological analysis to examine the bone structure (Fig. 4B). Transplantation of 10^3 to 10^5 control cells had a 100% success rate on bone formation (Fig. 4C). At 10^2 cells from control mice, ectopic bone tissue formed although at a lower frequency than with the higher number of cells (Fig. 4C). In contrast, ectopic bone tissue was not detected in kidneys transplanted with 10^2 to 10^3 Bmpr1a^{Ax2} cells, and only at 10^5 cells did all of the kidney capsules exhibit bone formation (Fig. 4C). Estimating stem cell frequency using Extreme Limiting Dilution Analysis (ELDA) software (*30*), we found the loss of *Bmpr1a* significantly decreases SuSC frequency in the P5 suture (Fig. 4C; control, 1 in 216 cells; Bmpr1a^{Ax2}, 1 in 23,572 cells, $P = 5.7 \times 10^{-6}$).

Furthermore, immunostaining analysis revealed a significant loss of Axin2$^+$ SuSCs in the Bmpr1a^{Ax2} suture (Fig. 4D; control, 4.9 ± 0.3%; Bmpr1a^{Ax2} 0.6 ± 0.2%, $P < 0.01$). These data suggested that Bmpr1a plays an essential role in the maintenance of SuSC stemness such that the loss of Bmpr1a induces their precocious differentiation and aberrant ossification in the suture midline, leading to craniosynostosis.

Preservation of SuSC stemness in culture

A protocol for maintaining SuSC stemness in vitro is needed because conventional culture methods for mesenchymal stromal cells do not preserve SuSC stemness. Sphere culture can maintain the properties of neural and mammary stem cells, recapitulating in vivo characteristics (*31*). We established a culture protocol for cells isolated from the suture mesenchyme (fig. S9A) that maintains stem cell characteristics. We found that the isolated suture cells formed primary (1°) spheres when grown in single-cell suspension culture at very low seeding density (fig. S9, B and C). When 1° spheres were dissociated into single cells, the cells formed secondary (2°) spheres (fig. S9D). For each passage, 10^4 cells were seeded and suture cell spheres continued to form without notable decreases in number for up to five passages, implying the presence of SuSCs with self-renewing ability (fig. S9E). The time-course analysis suggested that each sphere formed from a single cell (fig. S9, F to K). The average sphere size remained comparable in different passages (fig. S9L).

To determine the cellular origin of the sphere-forming cells, we used the Axin2$^{Cre\text{-}Dox}$; R26RTomato model (fig. S1B). Suture cells, isolated from the Axin2$^{Cre\text{-}Dox}$; R26RTomato mice with Dox treatment for 3 days from P7 to P10, were cultured in the absence of Dox. A small portion of cells was positive for Tomato at the beginning of the single-cell suspension culture (Fig. 5A, top row; 5 ± 0.3%, $n = 3$, means ± SEM). After 2 weeks, most spheres consisted of all Tomato$^+$ cells, suggesting that they derived from a single Axin2$^+$ cell with clonal expansion ability (Fig. 5, A and B). We did not detect chimeric spheres with a mixture of Tomato$^+$ and Tomato$^-$ cells, indicating that suture spheres are not formed by cell aggregation.

We evaluated the multipotency of the suture spheres by culturing the spheres under conditions that promote differentiation. These multipotency tests showed that 3° spheres differentiated into osteoblast cells and formed mineralized nodules or into chondrogenic cells (fig. S9, M to O). To examine the clonal expansion and bone-forming abilities of suture spheres in vivo, we performed kidney

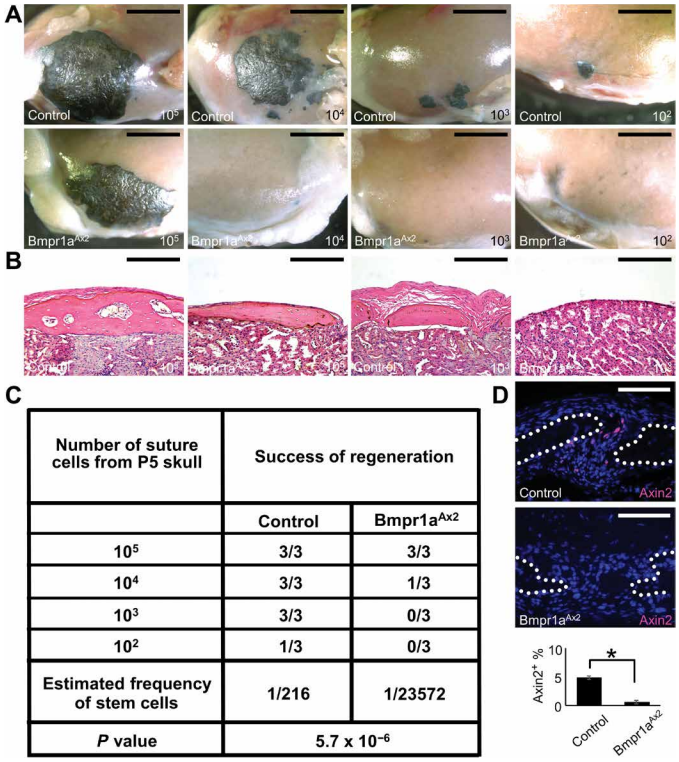

Number of suture cells from P5 skull	Success of regeneration	
	Control	Bmpr1a^{Ax2}
10^5	3/3	3/3
10^4	3/3	1/3
10^3	3/3	0/3
10^2	1/3	0/3
Estimated frequency of stem cells	1/216	1/23572
P value	5.7 x 10^{-6}	

Fig. 4. Bmpr1a regulates SuSCs and stem cell–dependent bone formation. (**A** to **C**) Kidney capsule transplantation with limiting dilution analysis of control and Bmpr1a^{Ax2} cells, isolated from the P5 suture mesenchyme of mice administered Dox from E16.5 to P3, to examine SuSC frequency ($n = 3$ mice per group). Control mice were Axin2-rtTA; Bmpr1a$^{Fx/Fx}$ or TRE-Cre; Bmpr1a$^{Fx/Fx}$ mice with Dox. Ectopic bone formation is assessed by von Kossa staining in whole mounts (A) and histology in sections (B). Scale bars, 4 mm (A) and 200 μm (B). Quantification of bone formation rate with transplantation of 10^5, 10^4, 10^3, and 10^2 cells with a quantitative estimation for stem cell frequency using ELDA software (C). (**D**) Immunostaining for Axin2 of sections of the P7 sagittal suture with quantification of the average percentage of Axin2$^+$ cells. Sections were counterstained with 4′,6-diamidino-2-phenylindole (DAPI). Broken lines define the calvarial bones (scale bars, 100 μm). Quantified data are from three mice per group and are presented as means ± SEM (*$P < 0.01$ by Student's *t* test).

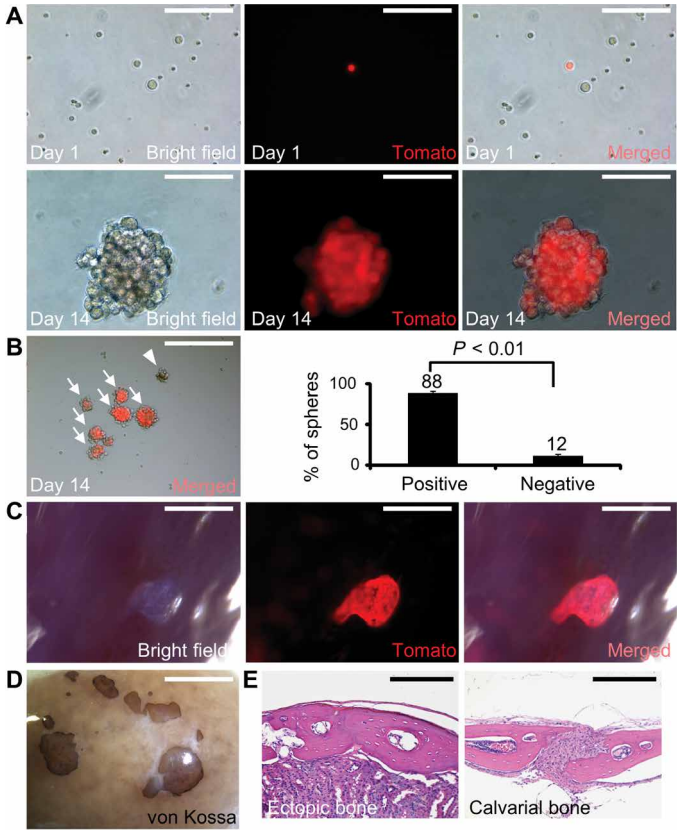

Fig. 5. SuSC stemness is preserved in sphere culture. (**A** and **B**) Genetic cell labeling with the Axin2$^{Cre-Dox}$; R26RTomato mouse model was used to trace the fate of Axin2$^+$ SuSCs in sphere culture. Dox was administered to Axin2$^{Cre-Dox}$; R26RTomato mice from P7 to P10. Panel (A) shows fluorescent images of Axin2$^+$ SuSCs on day 1 and day 14 of culture. Scale bars, 100 μm. Panel (B) shows the evaluation of the proportion of spheres derived from Axin2$^+$ cells (arrows) and Axin2$^-$ cells (arrowhead). The proportion of spheres derived from Axin2$^+$ and Axin2$^-$ cells was quantified ($P < 0.01$, $n = 3$, means ± SEM, Student's *t* test). Scale bar, 400 μm. (**C**) Whole-mount imaging of Tomato fluorescence of (Axin2$^+$-derived) SuSC spheres 4 weeks after transplantation into the kidney capsule. Scale bars, 1 mm. (**D**) Whole-mount von Kossa staining of ectopic bones generated by SuSC spheres 8 weeks after transplantation. (**E**) Comparison of ectopic bone grown from SuSC spheres 8 weeks after transplantation into a kidney capsule (left) and calvarial bone plate from a 2-month mouse skull (right). Sections were stained with hematoxylin and eosin. Scale bars, 200 μm. In (C) to (E), images are representatives of three independent experiments.

capsule transplantation analysis. We implanted 30 spheres, which were formed from cells isolated from the Axin2$^{Cre-Dox}$; R26RTomato suture, into the kidney capsule. The spheres successfully expanded, colonized, and engrafted (Fig. 5C). Like transplanted freshly isolated suture cells undergoing intramembranous ossification (*5*), the transplanted 1° spheres (Fig. 5, D and E) or 3° spheres (fig. S9, P to S) generated bone tissue resembling calvarial bones (Fig. 5E). The results indicated that the newly developed culture system preserves SuSC stemness and differentiation properties, enabling their analyses in an ex vivo setting.

Ex vivo characterization of SuSCs

Previous in vivo examination of mouse SuSCs at 1 month old, as well as our data for P3 suture mesenchyme (Fig. 3B), indicated their quiescence (*5*). These quiescent SuSCs should be included with our isolation procedure for sphere culture. To test whether a subpopulation of the isolated SuSCs exhibit quiescence in culture, we performed pulse-chase labeling analyses by labeling the cells in vivo and then chasing them in culture. Using the Axin2^{GFP} (Axin2-rtTA; TRE-H2BGFP) mouse model (fig. S1A), we performed a pulse-chase analysis to examine Axin2$^+$ SuSCs. *Axin2*-expressing cells were labeled in vivo with GFP by the administration of Dox from P7 to P10 (*5*). Suture cells were isolated at P10 and cultured in the absence of Dox for sphere formation. GFP analysis of 1° spheres revealed only a single cell with strong fluorescence intensity (Fig. 6A). Similar results were obtained in the subsequent 2° and 3° cultures (Fig. 6, B and C). Although 32% of the 1° spheres lacked any GFP$^+$ cells, all spheres found in the 2° and 3° passages contained one strongly GFP$^+$ cell (Fig. 6D). The presence of some GFP$^-$ spheres in the 1° culture is likely due to the presence of skeletal precursors with limited proliferation ability that only generate spheres in the 1° culture and not in the subsequent passages. We hypothesized that the persistent

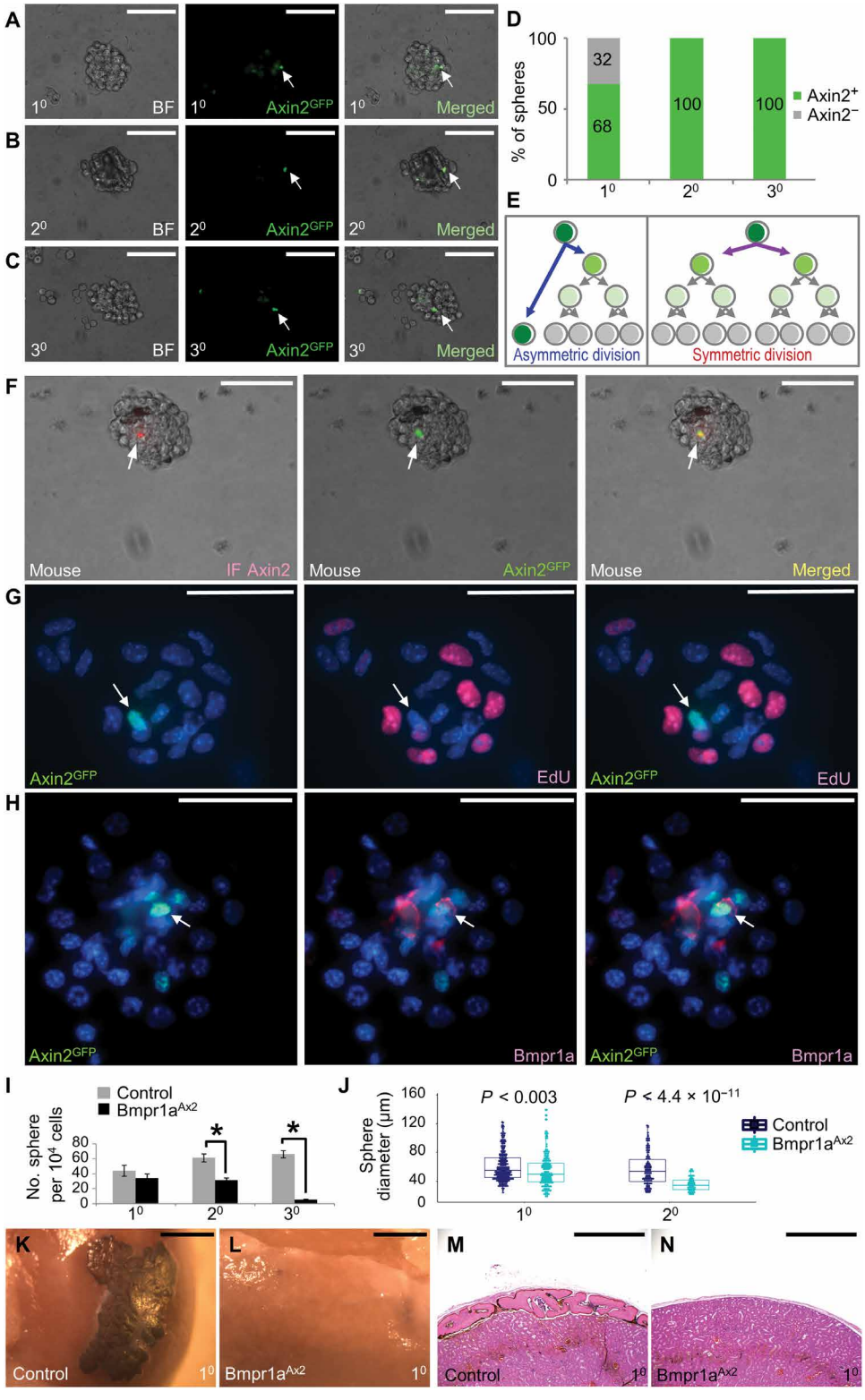

Fig. 6. Bmpr1a is essential for SuSC self-renewal. (**A** to **C**) Ex vivo pulse-chase labeling analysis of cells isolated from Axin2^{GFP} mouse sutures labeled in vivo from P7 to P10 by the administration of Dox and then cultured in the absence of Dox. Spheres from 1°, 2°, and 3° cultures were examined for the presence of cells with GFP fluorescence (arrows). BF, bright field. (**D**) Graph of the percentage of spheres with (Axin2$^+$) or without (Axin2$^-$) the label-retaining GFP$^+$ cell in the indicated passages. (**E**) Diagrams illustrating the distribution of GFP intensity in cells generated by the asymmetric or symmetric division of SuSCs. (**F** and **G**) Ex vivo pulse-chase labeling of Axin2$^+$ cells [as described for (A) to (C)] was followed by immunostaining for Axin2 (F) or incubation of cells with EdU to label proliferating cells (G) in the suture spheres. Arrows indicate a single GFP$^+$ label-retaining cell that is positive for Axin2 immunofluorescence (IF) (F) or is negative for EdU labeling (G). Scale bars, 100 μm (F) and 50 μm (G). (**H**) Ex vivo pulse-chase labeling of Axin2$^+$ cells [as described for (A) to (C)] was followed by immunostaining for Bmpr1a in the suture spheres. Arrows indicate a single GFP$^+$ label-retaining cell that is positive for Bmpr1a. Scale bars, 50 μm. (**I** and **J**) In vitro self-renewal was examined by serial culturing of spheres, and sphere number (I) and size (J) were evaluated in spheres from suture cells from control mice or Bmpr1a^{Ax2} mice. For sphere number, the data are presented as means ± SEM ($n = 3$; *$P < 0.05$, Student's t test). For sphere size, individual spheres are shown with the average (middle line), 75% tile (top line), and 25% tile (bottom line) values. Statistical significance was determined by the two-sided Student's t test [n values: 1° control, 236 spheres, and Bmpr1a^{Ax2}, 188 spheres; 2° control, 124 spheres, and Bmpr1a^{Ax2}, 66 spheres ($N = 3$ independent experiments)]. (**K** to **N**) Kidney capsules were transplanted with the 1° spheres cultured from control or Bmpr1a^{Ax2} cells, isolated from the P5 suture mesenchyme of mice administered Dox from E16.5 to P3 ($n = 3$ mice per group). Control mice were Axin2-rtTA; Bmpr1a$^{Fx/Fx}$ or TRE-Cre; Bmpr1a$^{Fx/Fx}$ mice with Dox. Tissue was evaluated by whole-mount von Kossa staining (K and L) and histological (M and N) analyses. Scale bars, 2 mm (K and L) and 800 μm (M and N).

presence of a single cell that is strongly GFP$^+$ arises from asymmetric division, whereas symmetric division dilutes the GFP signal (Fig. 6E). We confirmed that the GFP$^+$ cell was also positive for Axin2 by immunofluorescence analysis (Fig. 6F). Labeling the spheres for proliferating cells showed that the GFP$^+$ cell was not actively proliferating (Fig. 6G). These results support our hypothesis that SuSCs undergo asymmetric division in which one daughter cell remains undifferentiated, thus showing label-retaining ability, and the rest of the cells in the sphere arise from the other daughter cell (Fig. 6E).

A requirement of Bmpr1a for self-renewal and bone formation of SuSCs

Using ex vivo pulse-chase labeling analysis, we examined the distribution of Bmpr1a in the spheres. Spheres immunostained for Bmpr1a showed that this receptor is present in the GFP$^+$ cell and a few

neighboring cells (Fig. 6H). These results are consistent with our in vivo double-labeling analysis showing only partial overlap of the Bmpr1a and Axin2 reporter signals (fig. S2, C to E). Next, we examined the necessity of Bmpr1a for SuSC self-renewal using serial culture analysis. The culture of cells isolated from the P5 control and Bmpr1a^{Ax2} sutures showed comparable sphere formation in 1° cultures (Fig. 6I). However, the number of 2° and 3° spheres was significantly reduced in cultures from the mutant mice, suggesting that the self-renewing ability of SuSCs is compromised by the loss of *Bmpr1a* (Fig. 6I; $P < 0.05$, $n = 3$, means ± SEM, Student's t test). The size of the mutant spheres was also smaller compared to the control (Fig. 6J). Thus, the data indicated that Bmpr1a plays an essential role in SuSC self-renewal and maintenance of stemness properties in sphere culture.

Our prior study showed that SuSC self-renewal is linked to clonal expansion and bone regeneration in vivo, especially when a small number of cells are used for transplantation analysis (*5*). To test whether clonal expansion and osteogenic abilities are affected in *Bmpr1a*-deficient SuSCs, we implanted 30 spheres into the kidney capsule. In this assay, we used 1° spheres because of the impaired formation of the mutant spheres in subsequent passages (Fig. 6I). Ectopic bone formation mediated by Bmpr1a^{Ax2} 1° suture spheres was severely impaired (Fig. 6, K to N). In one of three transplants with mutant spheres, we detected a tiny area that stained with von Kossa.

To exclude potential noncell-autonomous effects on SuSCs that occur before isolation from the *Bmpr1a*-deficient mice using the Bmpr1a^{Ax2} model, we used suture cells isolated from Bmpr1a$^{Fx/Fx}$ mice, infected the cells in culture with lentivirus expressing GFP (control) or Cre, grew the cells until they formed spheres, and then used the 1° spheres for kidney capsule transplantation. The efficiency of lentivirus-mediated expression that had minimal toxicity was determined with lentivirus expressing RFP: At a multiplicity of infection (MOI) of 1, the expression seemed optimal without notable changes in sphere size or number (fig. S10, A to C). Cre-dependent deletion of *Bmpr1a* in suture spheres was highly efficient (fig. S10D) and drastically reduced the size of the generated bone tissue when transplanted into the kidney capsule (fig. S10, E to G; $P < 0.05$, $n = 3$, means ± SEM, Student's t test).

These results with those from the Bmpr1a^{Ax2} model suggested that Bmpr1a has two key roles: Bmpr1a supports asymmetric division and clonal expansion of SuSCs (Fig. 6) and bone formation of SuSCs in a cell-autonomous manner (Fig. 6 and fig. S10). Thus, the data indicated that Bmpr1a regulates not only SuSC self-renewal but also SuSC-mediated skeletogenesis.

Characterization of human SuSCs

To test for the existence of human SuSCs and our ability to isolate them and maintain them in culture, we obtained discarded tissue containing unfused sutures from patients with craniosynostosis undergoing surgical operations. First, we detected AXIN2$^+$ cells and BMPR1A$^+$ cells in the midline of human sutures by immunostaining of tissue sections (Fig. 7, A to C, and fig. S11). We determined that the isolated human suture cells grow into 1° spheres when cultured in single-cell suspension with very low seeding density (Fig. 7D). We obtained 2° and 3° spheres without notable decreases in number and size after serial replating (10^4 cells for 1° to 3°), indicating the presence of human SuSCs with self-renewing ability (Fig. 7, E and F). Human suture spheres stained for AXIN2 and colabeled with 5-ethynyl-2′-deoxyuridine (EdU) revealed that the majority of human suture spheres contains an AXIN2$^+$ cell which is not colocalized with EdU$^+$ proliferating cells (Fig. 7, G to I). These results indicated that human SuSCs are quiescent/slow-cycling cells and maintain their stemness through asymmetric division.

Last, implantation of human cells into mouse kidney capsules revealed the formation of ectopic bones positive for von Kossa staining in whole mounts and sections (Fig. 7, J to K) with an 80% success rate ($n = 5$). Our findings demonstrated successful isolation and culture of human SuSCs, a major hurdle to overcome for translational study.

Bone formation from mouse and human Bmpr1a-expressing cells

The important role of Bmpr1a in stem cell regulation and the overlap in Bmpr1a and Axin2 positivity (fig. S2E) prompted us to test its use as a cell surface marker for SuSC isolation. Using a specific antibody and fluorescence-activated cell sorting (FACS), we purified Bmpr1a^{High} from mouse (BMPR1A^{High} from human) and Bmpr1a/BMPR1A^{Low} cell populations from mouse/human sutures (Fig. 8A and fig. S12). Mouse suture cells were from P10 C57/BL6 mice; human cells were from discarded calvarial tissues containing unfused suture of patients with craniosynostosis. Successful bone formation was evident in the animal recipients with implantation of mouse Bmpr1a^{High} but not Bmpr1a^{Low} mouse suture cells (Fig. 8, B and C). Immunostaining of Osx identified osteoprogenitor cells surrounding the mineralized tissues generated by transplantation of mouse Bmpr1a^{High} (Fig. 8, D and F) cells. We achieved the same results with human BMPR1A^{High} suture cells (Fig. 8, G to L). The results indicated that Bmpr1a/BMPR1A functions as an SuSC marker. Furthermore, these results confirmed not only that Bmpr1a functionally regulates stem cell stemness that is essential for suture patency and craniosynostosis but also that SuSCs are included in the Bmpr1a^{High} cell population in both mice and humans.

DISCUSSION

This study provides evidence that Bmpr1a is essential for SuSC regulation. Loss of *Bmpr1a* in *Axin2*-expressing cells impaired SuSC self-renewal, clonal expansion, and osteogenic abilities. Thus, Bmpr1a was required for maintaining these functions associated with stem cell stemness, implying a role for this receptor in repressing differentiation or in promoting asymmetric cell division. A suppressive effect of BMP signaling on early osteogenesis is supported by prior reports showing that neonatal disruption of Bmpr1a or its ablation in osteoprogenitor cells increases the osteoblast cell number (*32*–*34*). Loss of *Bmpr1a* reduced Smad phosphorylation and enhanced the activation of p38 and Erk, suggesting that the balance of canonical and noncanonical BMP signaling cascades is altered in SuSCs. Alternatively, the inactivation caused hyperactivation of signaling downstream of the other BMP type I receptors. It has been proposed that Bmpr1a regulates this balance through modulation of Tak1 activity (*35*). Because Tak1 was not activated in the Bmpr1a^{Ax2} mutant, our findings suggested that a noncanonical pathway distinct from Tak1-mediated MAPK signaling is responsible for Bmpr1a-mediated SuSC stemness.

In the kidney capsule transplantation, only suture cells positive but not those negative for Axin2 can generate bones (*5*). This implies that skeletal stem cells included in the Axin2$^+$ cell population

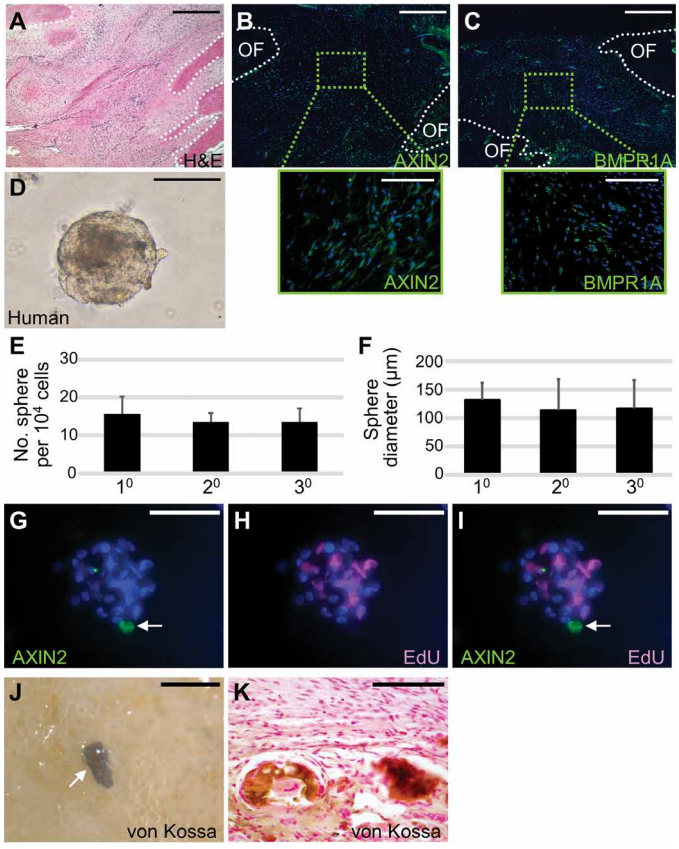

Fig. 7. Self-renewal and osteogenic ability of human SuSCs. (**A** to **C**) Sections of the 14-month-old human coronal suture were examined by hematoxylin and eosin (H&E) staining (A) or by immunostaining for AXIN2 (B) or BMPR1A (C). Broken lines define the calvarial bones at the osteogenic front. Scale bars, 500 μm in main images and 100 μm in enlarged images from (B) and (C). Images are representative of ≥5 individuals. (**D** to **F**) Characterization of spheres formed by cells isolated from human suture tissue. A representative primary sphere is shown in (D). Scale bar, 100 μm. Graphs of average number (E; $n = 5$, means ± SD) and size (F; $n = 5$, >15 spheres in each passage, means ± SD) of spheres formed by the indicated culture of human suture cells starting with 10^4 cells for each passage. (**G** to **I**) Immunostaining for AXIN2 (arrow) and EdU labeling of a human sphere. Scale bars, 100 μm. (**J** and **K**) Kidney capsules were transplanted with the 30 primary human spheres and evaluated by von Kossa staining of whole-mounts (J) and sections (K). Scale bars, 300 μm (J) and 100 μm (K). Data in (G) to (K) are representatives of at least five independent experiments.

have bone-forming ability in the kidney capsule. Even though there are osteogenic precursors or osteoblast cells within the $Axin2^-$ cell population, these cells are unable to form ectopic bones (*5*). The requirement for $Axin2^+$ cells for ectopic bone generation may explain why direct engraftment and replacement of damaged tissue are difficult to achieve in most cell-based therapies. The number of $Axin2^+$ cells is too few in most therapies, and osteoblasts, despite being the bone-forming cells in vivo, are ineffective for bone formation upon transplantation. For therapeutic success, the survival, engraftment, and expansion of the transplanted cells seem highly critical factors. Only stem cells have these properties, and we found that those properties are preserved by Bmpr1a using both an in vivo ablation model and a culture deletion model. Further elucidation of the regulatory mechanism underlying cell survival and engraftment promises important insight into Bmpr1a-mediated bone regeneration, leading to a previously unknown strategy for stem cell–based therapy.

SuSC-specific ablation of Bmpr1a resulted in precocious differentiation and suture fusion. Our findings revealed a previously unidentified etiology for craniosynostosis—stem cell depletion. This pathogenetic mechanism is distinct from other known mechanisms: cell proliferation, differentiation, and apoptosis, any of which cause excessive intramembranous ossification (*14*). It is also different from our previous report in which suture fusion can be caused by stem cell fate switching: SuSCs undergo chondrogenesis instead of osteoblastogenesis, leading to craniosynostosis mediated by ectopic endochondral ossification (*18*). Stem cell depletion has previously been associated with ossification deficiency that may be related to patients with Cole-Carpenter syndrome that exhibit wide-open midline sutures containing intrasutural bones (*36*). Intrasutural bone, which is also known as Wormian bone, occurs frequently in disorders with reduced cranial ossification and has been associated with craniosynostosis (*37*). The stem cell depletion mechanism that we identified should be explored in synostosis patients without the enhanced ossification phenotype.

Although skeletal stem cells residing in the suture were identified, their role in craniosynostosis was not investigated (*5*, *6*). Axin2 and Gli1 have been used to identify skeletal stem cells in the calvarium (*5*, *6*), but the deletion of *Bmpr1a* in $Gli1^+$ cells does not induce craniosynostosis, despite resulting in enhanced osteoblast proliferation and differentiation (*38*). This discrepancy may be attributed to the presence of Axin2 in a more restricted cell population in the suture midline (*5*, *6*). Also, Bmpr1a colocalizes with Axin2 but not Gli1 (*38*). Our results showed that $Axin2^+$ SuSCs undergo asymmetric division to maintain quiescence. We speculate that disruption of Bmpr1a-dependent regulation of SuSC quiescence is likely the trigger for craniosynostosis. We propose that because SuSC stemness is maintained by Bmpr1a, its deletion leads to aberrant ossification initiated at the suture midline. Therefore, craniosynostosis arises from skeletal stem cell deficiency.

Preserving stemness in vitro is critical for engineering bone tissue. Although sphere-forming cells from bone marrow have been reported, there is a lack of evidence regarding their in vivo origin and osteogenic ability (*39*–*41*). Whether their stemness is preserved in vitro remains unknown. We developed an ex vivo protocol to culture SuSCs for an extended period. The cultured SuSCs generated bone tissue upon implantation into an ectopic site. Furthermore, the SuSC culture provides an outstanding system for examination of skeletal stem cell characteristics, such as asymmetric division, cell fate determination, generation of skeletal progenitors, and skeletogenic differentiation. Thus, this system represents a tool for advancing stem cell–based therapy for bone regeneration and repair.

To support the translation of our research into humans, we identified human $BMPR1A^+$ SuSCs capable of generating ectopic bone tissue. Because Axin2 is an intracellular protein, it is essential to identify a surface marker for stem cell purification. The BMP antagonist Gremlin1 labels skeletal stem cells that contribute to endochondral ossification; however, the functional importance of Gremlin1 remains unclear (*8*). Our results demonstrated that Bmpr1a not only is a key regulator of SuSCs but also serves as a marker for their isolation. We showed that BMPR1A, which is also known as CD292 (*42*), can be used to isolate human or mouse suture cells that have skeletal stem cell properties for bone formation. The findings provide

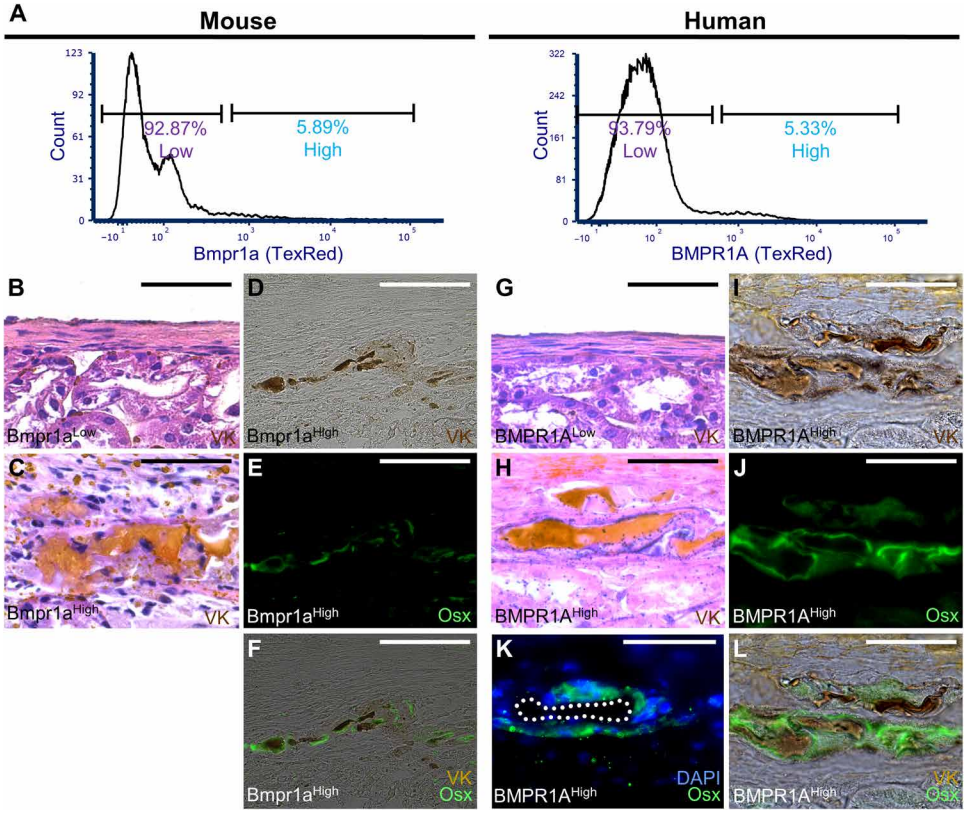

Fig. 8. The osteogenic ability of mouse Bmpr1a$^+$ and human BMPR1A$^+$ suture cells. (**A**) Cell sorter isolation of Bmpr1a/BMPR1A^{High} and Bmpr1a/BMPR1A^{Low} cell populations from P10 mouse or human suture mesenchymes. (**B** to **F**) Sorted mouse cells (5×10^3) were transplanted into kidney capsules and evaluated by von Kossa (VK) staining to identify bone tissue or immunostaining for Osx to identify osteoprogenitor cells. (**G** to **L**) Sorted human cells (5×10^3) were transplanted into kidney capsules and evaluated by von Kossa staining to identify bone tissue or immunostaining for Osx to identify osteoprogenitor cells. In (K), tissue was counterstained with DAPI, and the dotted area represents bone. Images are the representatives of at least five independent experiments. Scale bars, 50 μm (B and C and H to M) and 100 μm (D to F).

compelling evidence that BMPR1A positivity can be used for the purification of the human SuSC population.

There are some limitations of our study. Although we successfully maintained SuSC stemness in culture, this property was limited to five passages. Genetically based cell tracing shows that SuSCs maintain self-renewing ability for more than 1 year (*5*), suggesting potential improvement for long-term culture. Increasing stem cell numbers ex vivo is another improvement beneficial for translational implications. Although the transplanted SuSCs generate intramembranous bones highly reminiscent of calvarial bones, no suture-like structure is formed from the transplanted cells in the kidney capsule. This may relate to a lack of niche cells required for suture generation. We speculate that the inclusion of SuSC niche cells is essential for ectopic suture generation.

Our SuSC study promotes future niche cell identification and isolation, leading to the prevention of suture resynostosis in surgical patients or possibly the development of a preventive procedure for premature suture closure as an alternative to surgery for patients with craniosynostosis. Further elucidation of the mechanism underlying SuSC regulation and SuSC-mediated regeneration promise advancements in our knowledge base of congenital deformity and skeletal repair.

METHODS

Study design

This study was designed to identify regulators of SuSCs. Using a genomic approach, we found that BMP signaling was potentially involved in SuSC regulation. We generated loss-of-function mouse models to individually examine three BMP type I receptors, revealing that Bmpr1a was essential for SuSC-mediated calvarial morphogenesis. We used an inducible knockout system to specifically disrupt *Bmpr1a* in Axin2$^+$ SuSCs in developing mice and evaluated the effect of disruption on suture fusion and studied the mechanism of the aberrant suture closure. To test whether stem cell depletion caused precocious differentiation that mediated aberrant suture closure, we examined stemness, self-renewal, quiescence, stem cell frequency, proliferation, clonal expansion, and bone-generating ability of SuSCs using ex vivo culture and in vivo transplantation assays. To provide translation to humans, we analyzed a human SuSC population and determined whether BMPR1A served as a cell surface marker for isolation of both mouse and human SuSCs with characteristics of skeletal stem cells. To ensure scientific reproducibility, all studies were performed multiple times with proper controls, including wild-type mice or mice carrying appropriate transgene(s). Mice of both sexes were examined because of the potential sensitivity of skeletogenesis to sex hormones. For mouse studies, at least three or five mice were used for each group. For culture studies and transplantation studies, at least three to five independent experiments were performed. Human samples were obtained from patients with nonsyndromic synostosis with at least five independent samples used for this study. The analysis of samples by μCT was performed by a technician who was blinded to the condition. No randomization, statistical method to predetermine the sample size, or inclusion/exclusion-defining criteria for samples were used.

Animals and models

The Axin2-rtTA, TRE-H2BGFP, TRE-Cre, R26RTomato, Bmpr1a^{Fx}, Acvr1^{Fx}, Bmpr1b$^{-/-}$, severe combined immunodeficient mouse strains, and genotyping methods were reported previously (*18*, *25*, *43*–*51*). To create the Axin2^{GFP} strain (*18*, *52*), mice carrying Axin2-rtTA and TRE-H2BGFP transgenes were obtained and treated with Dox [2 mg/ml plus sucrose (50 mg/ml)] for 3 days as described (*43*, *44*, *49*). The Axin2$^{Cre\text{-}Dox}$ mouse strain was generated by obtaining mice carrying Axin2-rtTA and TRE-Cre transgenes. The Axin2$^{Cre\text{-}Dox}$ mice were then crossed with Bmpr1a^{Fx}, Acvr1^{Fx}, and R26RTomato mice to obtain Bmpr1a^{Ax2}, Acvr1^{Ax2}, and Axin2$^{Cre\text{-}Dox}$; R26RTomato mouse, respectively. The expression of Cre in the

Axin2-expressing cells was then induced by Dox treatment (*18*, *53*). Both male and female mice were used in this study. Care and use of experimental animals described in this work comply with guidelines and policies of the University Committee on Animal Resources at the University of Rochester.

Cell isolation and purification

Primary suture mesenchymal cells containing SuSCs were isolated from mouse calvaria as described (*5*). Briefly, an about 1.5-mm-width tissue containing the sagittal suture and the adjacent parietal bones was dissected, and the suture was separated from the parietal bone parts. Suture parts were incubated with 0.2% collagenase in phosphate-buffered saline (PBS) (pH 7.0 to 7.6, 21-031-CV, Corning) at 37°C for 1.5 hours. The dissociated cells were filtered using Cell Strainer 40-μm Nylon (352340, Falcon), and then resuspended in Dulbecco's modified Eagle's medium (DMEM) for transplantation analysis, in DMEM containing 5% fetal bovine serum (FBS) for cell sorting, or in DMEM containing insulin (25 μg/ml), transferrin (100 μg/ml), 20 nM progesterone, 30 nM sodium selenite, 60 nM putrescine, epidermal growth factor (20 ng/ml), basic FGF (20 ng/ml), B27 supplement (20 ng/ml), and 1% penicillin-streptomycin for sphere culture.

For in vitro culture as spheres, cells were grown for 7 to 10 days in ultralow attachment surface plates (2023-03-23, Corning) during which time the cells formed spheres (1°). The spheres were dissociated with 0.25% trypsin-EDTA and seeded as a single-cell suspension in ultralow attachment surface plates for the culture of the next passage (2°). This process of dissociation and replating was repeated for up to five passages (5°). For differentiation, the spheres were transferred to 24-well plates with treated surfaces (662160, Greiner Bio-One, Monroe, NC) to enhance attachment and cultured in differentiation α-MEM medium containing ascorbic acid (50 μg/ml) and 4 mM β-glycerophosphate for 3 weeks.

For human suture cell isolation, we obtained calvarial discards containing unfused suture from patients with nonsyndromic craniosynostosis (3 to 14 months). Bone fragments were removed to obtain the suture mesenchyme and the tissue was incubated with 0.2% collagenase in PBS (pH 7.0 to 7.6, 21-031-CV, Corning) for 1.5 hours at 37°C. The dissociated cells were then filtered through a 40-μm strainer, followed by resuspension in DMEM containing 20% FBS for sphere culture or in PBS containing 3% FBS for cell purification.

To purify $Bmpr1a^+$ and $Bmpr1a^-$ cell populations, freshly isolated suture cells were stained with primary mouse monoclonal Bmpr1a antibody (MA5-17036, Thermo Fisher Scientific, Waltham, MA), followed by sorting according to the intensity of secondary antibody-conjugated Texas Red using FACSAria II (BD Biosciences, San Jose, CA). The specificity of this Bmpr1a antibody for the isolation of cells with high amounts of Bmpr1a was determined by FACS (fig. S12).

Kidney capsule transplantation

The transplantation of freshly isolated suture cells or cultured sphere cells into the kidney capsule was performed as described (*5*). Freshly isolated cells were obtained from P5 mice. For limiting dilution analysis, 10^2 to 10^5 cells were transplanted. The frequency of stem cells was calculated with ELDA software (http://bioinf.wehi.edu.au/software/elda/) with validation of the likelihood ratio test for a single-hit model (*30*). Spheres were tested from 1° and 3° passages by transplanting 30 spheres per kidney capsule.

Staining and analysis

Skull preparation, fixation, and embedding for paraffin and frozen sections were performed as described (*16*, *18*, *53*, *54*). Samples were subject to hematoxylin/eosin staining for histology, Goldner's trichrome staining, GFP analysis, β-gal staining, van Kossa staining, or immunological staining with avidin:biotinylated enzyme complex (*16*, *18*, *43*, *44*, *54*–*58*). For antigen retrieval, samples were incubated with antigen unmasking solution (H3300, Vector) in pressure cooking for 10 min or 20 mM tris-HCl (pH 9) for 16 hours at 70°C. For in vitro deletion of Bmpr1a, cells isolated from mouse $Bmpr1a^{Fx/Fx}$ suture were infected by Lenti-GFP or Lenti-Cre viruses (MOI = 1). The whole-mount von Kossa staining, immunological staining, in situ hybridization, and double labeling analyses were performed as described (*5*, *54*, *59*). For double labeling of von Kossa staining and immunostaining, samples were fixed with 2% paraformaldehyde and 0.02% NP-40 for 1 hour at room temperature, followed by incubation with 1% silver nitrate under ultraviolet light for 30 min and with 5% sodium thiosulfate for 5 min. Then, the stained samples were processed for paraffin sections and subsequent immunological staining. To detect proliferating cells, EdU was added to the sphere for 16 hours after 4-day culture, followed by attachment using Cytospin (Thermo Fisher Scientific). After fixing with 95% ethanol for 5 min on ice and 2% paraformaldehyde for 20 min at room temperature, the spheres were treated with 0.5% Triton X-100 for 10 min and incubated with EdU reaction buffer for 30 min according to the manufacturer's protocol (Thermo Fisher Scientific). Rabbit polyclonal antibodies Osx (ab22552, Abcam, Cambridge, MA; 1:200), Bmpr1a (ABP-PAB-10536, Allele, San Diego, CA; 1:100), phospho-Tak1 (arb191688, Biorbyt, St. Louis, MO; 1:200), phospho-ERK1/2 (4370, Cell Signaling Technology, 1:50); rabbit monoclonal antibodies Ki67 (RM-9106, Thermo Fisher Scientific; 1:200), Axin2 (2151, Cell Signaling Technology; 1:500), phospho-p38 MAPK (4511, Cell Signaling Technology, 1:200), and phospho-JNK (4668, Cell Signaling Technology, 1:100) were used for immunostaining. The Bmpr1a antibody (MA5-17036, Thermo Fisher Scientific, 1:200) was used for FACS and immunostaining studies. Images were taken using a Zeiss Axio Observer microscope (Carl Zeiss, Thornwood, NY) or Leica DM2500 microscope with a DFC7000T digital imaging system (Leica Biosystems Inc., Buffalo Grove, IL).

Statistical analysis

R software version 3.2.1 or Microsoft Excel 2010 was used for statistical analysis. The significance was determined by two-sided Student's *t* tests. A *P* value of less than 0.05 was considered statistically significant. Before performing the *t* tests, the normality of the data distribution was first validated by the Shapiro-Wilk normality test. The activity of signaling pathways in SuSCs was estimated by the active *z* score using IPA software (Ingenuity Systems). Statistical data were presented as means ± SEM or SD. The stem cell frequency was examined by ELDA software (http://bioinf.wehi.edu.au/software/elda/) with validation of the likelihood ratio test for a single-hit model (*30*). Individual subject-level data are provided in data file S1.

SUPPLEMENTARY MATERIALS

stm.sciencemag.org/cgi/content/full/13/583/eabb4416/DC1

Fig. S1. Mouse genetic models for the identification of Axin2-expressing cells and their derivatives.

Fig. S2. Enhanced BMP signaling in suture stem cells.

Fig. S3. The efficacy of the Cre-mediated ablation of *Bmpr1a* and Bmpr1a antibody specificity.

Fig. S4. Effects of Bmpr1a loss of function on the skull.

Fig. S5. Multiple suture synostoses in skulls of mice with SuSC-specific deletion of *Bmpr1a*.
Fig. S6. Identification by μCT analysis of multiple suture synostosis in skulls of mice with SuSC-specific deletion of *Bmpr1a*.
Fig. S7. Chondrocyte analysis in Bmpr1a^{Ax2} mice.
Fig. S8. Effect of *Bmpr1a* ablation on signaling pathways in the developing suture.
Fig. S9. Ex vivo culture and differentiation of SuSCs.
Fig. S10. Lentiviral gene delivery to examine the loss of *Bmpr1a* in sphere-mediated bone formation.
Fig. S11. Identification of cells positive for AXIN2 and BMPR1A in the human lambdoid suture.
Fig. S12. Purification of mouse and human Bmpr1a/BMPR1A-expressing cells.
Data file S1. Individual subject-level data.

View/request a protocol for this paper from *Bio-protocol*.

REFERENCES AND NOTES

1. C. Mauffrey, B. T. Barlow, W. Smith, Management of segmental bone defects. *J. Am. Acad. Orthop. Surg.* **23**, 143–153 (2015).
2. P. Hernigou, A. Poignard, F. Beaujean, H. Rouard, Percutaneous autologous bone-marrow grafting for nonunions. Influence of the number and concentration of progenitor cells. *J. Bone Joint Surg. Am.* **87**, 1430–1437 (2005).
3. D. D. Lo, D. T. Montoro, M. Grova, J. S. Hyun, M. T. Chung, D. C. Wan, M. T. Longaker, Stem cell–based bioengineering of craniofacial bone, in *Stem Cells in Craniofacial Development and Regeneration*, G. T.-J. Huang, I. Thesleff, Eds. (Wiley, 2013), pp. 379–394.
4. N. J. Panetta, D. M. Gupta, M. T. Longaker, Bone regeneration and repair. *Curr. Stem Cell Res. Ther.* **5**, 122–128 (2010).
5. T. Maruyama, J. Jeong, T. J. Sheu, W. Hsu, Stem cells of the suture mesenchyme in craniofacial bone development, repair and regeneration. *Nat. Commun.* **7**, 10526 (2016).
6. H. Zhao, J. Feng, T. V. Ho, W. Grimes, M. Urata, Y. Chai, The suture provides a niche for mesenchymal stem cells of craniofacial bones. *Nat. Cell Biol.* **17**, 386–396 (2015).
7. C. K. F. Chan, E. Y. Seo, J. Y. Chen, D. Lo, A. M. Ardle, R. Sinha, R. Tevlin, J. Seita, J. Vincent-Tompkins, T. Wearda, W.-J. Lu, K. Senarath-Yapa, M. T. Chung, O. Marecic, M. Tran, K. S. Yan, R. Upton, G. G. Walmsley, A. S. Lee, D. Sahoo, C. J. Kuo, I. L. Weissman, M. T. Longaker, Identification and specification of the mouse skeletal stem cell. *Cell* **160**, 285–298 (2015).
8. D. L. Worthley, M. Churchill, J. T. Compton, Y. Tailor, M. Rao, Y. Si, D. Levin, M. G. Schwartz, A. Uygur, Y. Hayakawa, S. Gross, B. W. Renz, W. Setlik, A. N. Martinez, X. Chen, S. Nizami, H. G. Lee, H. P. Kang, J.-M. Caldwell, S. Asfaha, C. B. Westphalen, T. Graham, G. Jin, K. Nagar, H. Wang, M. A. Kheirbek, A. Kolhe, J. Carpenter, M. Glaire, A. Nair, S. Renders, N. Manieri, S. Muthupalani, J. G. Fox, M. Reichert, A. S. Giraud, R. F. Schwabe, J.-P. Pradere, K. Walton, A. Prakash, D. Gumucio, A. K. Rustgi, T. S. Stappenbeck, R. A. Friedman, M. D. Gershon, P. Sims, T. Grikscheit, F. Y. Lee, G. Karsenty, S. Mukherjee, T. C. Wang, Gremlin 1 identifies a skeletal stem cell with bone, cartilage, and reticular stromal potential. *Cell* **160**, 269–284 (2015).
9. P. T. Newton, L. Li, B. Zhou, C. Schweingruber, M. Hovorakova, M. Xie, X. Sun, L. Sandhow, A. V. Artemov, E. Ivashkin, S. Suter, V. Dyachuk, M. El Shahawy, A. Gritli-Linde, T. Bouderlique, J. Petersen, A. Mollbrink, J. Lundeberg, G. Enikolopov, H. Qian, K. Fried, M. Kasper, E. Hedlund, I. Adameyko, L. Savendahl, A. S. Chagin, A radical switch in clonality reveals a stem cell niche in the epiphyseal growth plate. *Nature* **567**, 234–238 (2019).
10. K. Mizuhashi, W. Ono, Y. Matsushita, N. Sakagami, A. Takahashi, T. L. Saunders, T. Nagasawa, H. M. Kronenberg, N. Ono, Resting zone of the growth plate houses a unique class of skeletal stem cells. *Nature* **563**, 254–258 (2018).
11. B. O. Zhou, R. Yue, M. M. Murphy, J. G. Peyer, S. J. Morrison, Leptin-receptor-expressing mesenchymal stromal cells represent the main source of bone formed by adult bone marrow. *Cell Stem Cell* **15**, 154–168 (2014).
12. D. M. Ornitz, P. J. Marie, Fibroblast growth factor signaling in skeletal development and disease. *Genes Dev.* **29**, 1463–1486 (2015).
13. C. K. F. Chan, C.-C. Chen, C. A. Luppen, J.-B. Kim, A. T. DeBoer, K. Wei, J. A. Helms, C. J. Kuo, D. L. Kraft, I. L. Weissman, Endochondral ossification is required for haematopoietic stem-cell niche formation. *Nature* **457**, 490–494 (2009).
14. L. A. Opperman, Cranial sutures as intramembranous bone growth sites. *Dev. Dyn.* **219**, 472–485 (2000).
15. A. O. M. Wilkie, G. M. Morriss-Kay, Genetics of craniofacial development and malformation. *Nat. Rev. Genet.* **2**, 458–468 (2001).
16. H.-M. Ivy Yu, B. Jerchow, T.-J. Sheu, B. Liu, F. Costantini, J. E. Puzas, W. Birchmeier, W. Hsu, The role of Axin2 in calvarial morphogenesis and craniosynostosis. *Development* **132**, 1995–2005 (2005).
17. E. Yilmaz, E. Mihci, B. Guzel Nur, O. M. Alper, A novel *AXIN2* gene mutation in sagittal synostosis. *Am. J. Med. Genet. A* **176**, 1976–1980 (2018).
18. T. Maruyama, A. J. Mirando, C.-X. Deng, W. Hsu, The balance of WNT and FGF signaling influences mesenchymal stem cell fate during skeletal development. *Sci. Signal.* **3**, ra40 (2010).
19. A. Krämer, J. Green, J. Pollard Jr., S. Tugendreich, Causal analysis approaches in Ingenuity Pathway Analysis. *Bioinformatics* **30**, 523–530 (2014).
20. X. Li, X. Cao, BMP signaling and skeletogenesis. *Ann. N. Y. Acad. Sci.* **1068**, 26–40 (2006).
21. J. Massague, TGF-β signal transduction. *Annu. Rev. Biochem.* **67**, 753–791 (1998).
22. Y. Mishina, A. Suzuki, N. Ueno, R. R. Behringer, Bmpr encodes a type I bone morphogenetic protein receptor that is essential for gastrulation during mouse embryogenesis. *Genes Dev.* **9**, 3027–3037 (1995).
23. Z. Gu, E. M. Reynolds, J. Song, H. Lei, A. Feijen, L. Yu, W. He, D. T. MacLaughlin, J. van den Eijnden-van Raaij, P. K. Donahoe, E. Li, The type I serine/threonine kinase receptor ActRIA (ALK2) is required for gastrulation of the mouse embryo. *Development* **126**, 2551–2561 (1999).
24. Y. Mishina, R. Crombie, A. Bradley, R. R. Behringer, Multiple roles for activin-like kinase-2 signaling during mouse embryogenesis. *Dev. Biol.* **213**, 314–326 (1999).
25. S. E. Yi, A. Daluiski, R. Pederson, V. Rosen, K. M. Lyons, The type I BMP receptor BMPRIB is required for chondrogenesis in the mouse limb. *Development* **127**, 621–630 (2000).
26. H. Williams, Lumps, bumps and funny shaped heads. *Arch. Dis. Child. Educ. Pract. Ed.* **93**, 120–128 (2008).
27. S. Nakata, Relationship between the development and growth of cranial bones and masticatory muscles in postnatal mice. *J. Dent. Res.* **60**, 1440–1450 (1981).
28. B. L. Hogan, Bone morphogenetic proteins: multifunctional regulators of vertebrate development. *Genes Dev.* **10**, 1580–1594 (1996).
29. M. S. Rahman, N. Akhtar, H. M. Jamil, R. S. Banik, S. M. Asaduzzaman, TGF-β/BMP signaling and other molecular events: Regulation of osteoblastogenesis and bone formation. *Bone Res* **3**, 15005 (2015).
30. Y. Hu, G. K. Smyth, ELDA: Extreme limiting dilution analysis for comparing depleted and enriched populations in stem cell and other assays. *J. Immunol. Methods* **347**, 70–78 (2009).
31. E. Pastrana, V. Silva-Vargas, F. Doetsch, Eyes wide open: A critical review of sphere-formation as an assay for stem cells. *Cell Stem Cell* **8**, 486–498 (2011).
32. J. Lim, Y. Shi, C. M. Karner, S.-Y. Lee, W.-C. Lee, G. He, F. Long, Dual function of Bmpr1a signaling in restricting preosteoblast proliferation and stimulating osteoblast activity in mouse. *Development* **143**, 339–347 (2016).
33. J. Zhang, C. Niu, L. Ye, H. Huang, X. He, W. G. Tong, J. Ross, J. Haug, T. Johnson, J. Q. Feng, S. Harris, L. M. Wiedemann, Y. Mishina, L. Li, Identification of the haematopoietic stem cell niche and control of the niche size. *Nature* **425**, 836–841 (2003).
34. N. Kamiya, L. Ye, T. Kobayashi, Y. Mochida, M. Yamauchi, H. M. Kronenberg, J. Q. Feng, Y. Mishina, BMP signaling negatively regulates bone mass through sclerostin by inhibiting the canonical Wnt pathway. *Development* **135**, 3801–3811 (2008).
35. H.-Y. Kua, H. Liu, W. F. Leong, L. Li, D. Jia, G. Ma, Y. Hu, X. Wang, J. F. L. Chau, Y.-G. Chen, Y. Mishina, S. Boast, J. Yeh, L. Xia, G.-Q. Chen, L. He, S. P. Goff, B. Li, c-Abl promotes osteoblast expansion by differentially regulating canonical and non-canonical BMP pathways and p16^{INK4a} expression. *Nat. Cell Biol.* **14**, 727–737 (2012).
36. D. J. Amor, R. Savarirayan, A. S. Schneider, A. Bankier, New case of Cole-Carpenter syndrome. *Am. J. Med. Genet.* **92**, 273–277 (2000).
37. P. A. Sanchez-Lara, J. M. Graham Jr., A. V. Hing, J. Lee, M. Cunningham, The morphogenesis of wormian bones: A study of craniosynostosis and purposeful cranial deformation. *Am. J. Med. Genet. A* **143A**, 3243–3251 (2007).
38. Y. Guo, Y. Yuan, L. Wu, T.-V. Ho, J. Jing, H. Sugii, J. Li, X. Han, J. Feng, C. Guo, Y. Chai, BMP-IHH-mediated interplay between mesenchymal stem cells and osteoclasts supports calvarial bone homeostasis and repair. *Bone Res* **6**, 30 (2018).
39. J. Isern, B. Martín-Antonio, R. Ghazanfari, A. M. Martín, J. A. López, R. del Toro, A. Sánchez-Aguilera, L. Arranz, D. Martín-Pérez, M. Suárez-Lledó, P. Marín, M. Van Pel, W. E. Fibbe, J. Vázquez, S. Scheding, Á. Urbano-Ispizúa, S. Méndez-Ferrer, Self-renewing human bone marrow mesenspheres promote hematopoietic stem cell expansion. *Cell Rep.* **3**, 1714–1724 (2013).
40. M. Shiota, T. Heike, M. Haruyama, S. Baba, A. Tsuchiya, H. Fujino, H. Kobayashi, T. Kato, K. Umeda, M. Yoshimoto, T. Nakahata, Isolation and characterization of bone marrow-derived mesenchymal progenitor cells with myogenic and neuronal properties. *Exp. Cell Res.* **313**, 1008–1023 (2007).
41. S. Debnath, A. R. Yallowitz, J. McCormick, S. Lalani, T. Zhang, R. Xu, N. Li, Y. Liu, Y. S. Yang, M. Eiseman, J.-H. Shim, M. Hameed, J. H. Healey, M. P. Bostrom, D. A. Landau, M. B. Greenblatt, Discovery of a periosteal stem cell mediating intramembranous bone formation. *Nature* **562**, 133–139 (2018).
42. P. Engel, L. Boumsell, R. Balderas, A. Bensussan, V. Gattei, V. Horejsi, B.-Q. Jin, F. Malavasi, F. Mortari, R. Schwartz-Albiez, H. Stockinger, M. C. van Zelm, H. Zola, G. Clark, CD nomenclature 2015: Human leukocyte differentiation antigen workshops as a driving force in immunology. *J. Immunol.* **195**, 4555–4563 (2015).
43. H.-M. Ivy Yu, B. Liu, F. Costantini, W. Hsu, Impaired neural development caused by inducible expression of Axin in transgenic mice. *Mech. Dev.* **124**, 146–156 (2007).
44. H.-M. Ivy Yu, B. Liu, S.-Y. Chiu, F. Costantini, W. Hsu, Development of a unique system for spatiotemporal and lineage-specific gene expression in mice. *Proc. Natl. Acad. Sci. U.S.A.* **102**, 8615–8620 (2005).

45. Y. Mishina, M. C. Hanks, S. Miura, M. D. Tallquist, R. R. Behringer, Generation of *Bmpr/Alk3* conditional knockout mice. *Genesis* **32**, 69–72 (2002).
46. M. Dudas, S. Sridurongrit, A. Nagy, K. Okazaki, V. Kaartinen, Craniofacial defects in mice lacking BMP type I receptor Alk2 in neural crest cells. *Mech. Dev.* **121**, 173–182 (2004).
47. L. Madisen, T. A. Zwingman, S. M. Sunkin, S. W. Oh, H. A. Zariwala, H. Gu, L. L. Ng, R. D. Palmiter, M. J. Hawrylycz, A. R. Jones, E. S. Lein, H. Zeng, A robust and high-throughput Cre reporting and characterization system for the whole mouse brain. *Nat. Neurosci.* **13**, 133–140 (2010).
48. T. Tumbar, G. Guasch, V. Greco, C. Blanpain, W. E. Lowry, M. Rendl, E. Fuchs, Defining the epithelial stem cell niche in skin. *Science* **303**, 359–363 (2004).
49. W. Hsu, A. J. Mirando, H.-M. Ivy Yu, Manipulating gene activity in Wnt1-expressing precursors of neural epithelial and neural crest cells. *Dev. Dyn.* **239**, 338–345 (2010).
50. E. O. Maruyama, H.-M. Ivy Yu, M. Jiang, J. Fu, W. Hsu, Gpr177 deficiency impairs mammary development and prohibits Wnt-induced tumorigenesis. *PLOS ONE* **8**, e56644 (2013).
51. H. J. Snippert, L. G. van der Flier, T. Sato, J. H. van Es, M. van den Born, C. Kroon-Veenboer, N. Barker, A. M. Klein, J. van Rheenen, B. D. Simons, H. Clevers, Intestinal crypt homeostasis results from neutral competition between symmetrically dividing Lgr5 stem cells. *Cell* **143**, 134–144 (2010).
52. J. Fu, M. Jiang, A. J. Mirando, H.-M. Ivy Yu, W. Hsu, Reciprocal regulation of Wnt and Gpr177/mouse Wntless is required for embryonic axis formation. *Proc. Natl. Acad. Sci. U.S.A.* **106**, 18598–18603 (2009).
53. A. J. Mirando, T. Maruyama, J. Fu, H. M. Ivy Yu, W. Hsu, β-catenin/cyclin D1 mediated development of suture mesenchyme in calvarial morphogenesis. *BMC Dev. Biol.* **10**, 116 (2010).
54. T. Maruyama, M. Jiang, W. Hsu, Gpr177, a novel locus for bone mineral density and osteoporosis, regulates osteogenesis and chondrogenesis in skeletal development. *J. Bone Miner. Res.* **28**, 1150–1159 (2013).
55. S.-Y. Chiu, N. Asai, F. Costantini, W. Hsu, SUMO-specific protease 2 is essential for modulating p53-Mdm2 in development of trophoblast stem cell niches and lineages. *PLOS Biol.* **6**, e310 (2008).
56. J. Fu, W. Hsu, Epidermal Wnt controls hair follicle induction by orchestrating dynamic signaling crosstalk between the epidermis and dermis. *J. Invest. Dermatol.* **133**, 890–898 (2013).
57. H. K. Russell Jr., A modification of Movat's pentachrome stain. *Arch. Pathol.* **94**, 187–191 (1972).
58. J. Fu, H.-M. Ivy Yu, S.-Y. Chiu, A. J. Mirando, E. O. Maruyama, J.-G. Cheng, W. Hsu, Disruption of SUMO-specific protease 2 induces mitochondria mediated neurodegeneration. *PLOS Genet.* **10**, e1004579 (2014).
59. T. Maruyama, M. Jiang, A. Abbott, H.-M. Ivy Yu, Q. Huang, M. Chrzanowska-Wodnicka, E. I. Chen, W. Hsu, Rap1b is an effector of Axin2 regulating crosstalk of signaling pathways during skeletal development. *J. Bone Miner. Res.* **32**, 1816–1828 (2017).

Acknowledgments: We thank Y. Mishina, K. Lyons, and V. Kaartinen for providing *Bmpr1a*, *Bmpr1b*, and *Acvr1* modified mouse strains, respectively, and J. Lopes, J. Martinez, C. Tang, Flow Cytometry Core, and Biomechanics and Multimodal Tissue Imaging Core for assistance. Editorial services were provided by N. R. Gough (BioSerendipity LLC, Elkridge, MD). **Funding:** This work is supported by the National Institutes of Health (DE15654 and DE269369) and NYSTEM (C029558) to W.H. **Author contributions:** T.M., K.N., and W.H. conceived and designed the experiments. T.M. and W.H. wrote the paper. T.M., R.S., A.B., L.D., C.C., H.-M.I.Y., C.M., and W.H. performed the experiments and analyzed the data. **Competing interests:** The authors declare that they have no competing financial interests. **Data and materials availability:** All data associated with this study are present in the paper or the Supplementary Materials. $Bmpr1a^{Fx}$ mouse strain is covered by a material transfer agreement with the National Institute of Environmental Health Sciences. Microarray data from three biological replicates of $Axin2^{+}$ and $Axin2^{-}$ mouse suture cells are available in Gene Expression Omnibus (GSE74849: https://ncbi.nlm.nih.gov/geo/). Correspondence and requests for materials should be addressed to wei_hsu@urmc.rochester.edu and wei_hsu@icloud.com.

Submitted 24 February 2020
Resubmitted 19 October 2020
Accepted 12 February 2021
Published 3 March 2021
10.1126/scitranslmed.abb4416

Citation: T. Maruyama, R. Stevens, A. Boka, L. DiRienzo, C. Chang, H.-M. I. Yu, K. Nishimori, C. Morrison, W. Hsu, BMPR1A maintains skeletal stem cell properties in craniofacial development and craniosynostosis. *Sci. Transl. Med.* **13**, eabb4416 (2021).

Science Translational Medicine

BMPR1A maintains skeletal stem cell properties in craniofacial development and craniosynostosis

Takamitsu MaruyamaRonay StevensAlan BokaLaura DiRienzoConnie ChangHsiao-Man Ivy YuKatsuhiko NishimoriClinton MorrisonWei Hsu

Sci. Transl. Med., 13 (583), eabb4416. • DOI: 10.1126/scitranslmed.abb4416

Signaling and suture stem cells

Suture stem cells give rise to craniofacial bone, and premature suture closure (craniosynostosis) is a common congenital deformity. Here, Maruyama *et al.* studied the role of bone morphogenetic protein (BMP) signaling in suture stem cell dysregulation and craniosynostosis. They found that deletion of BMP type I receptor, *Bmpr1a*, in suture stem cells caused craniofacial abnormalities in mice, including abnormal ossification and suture closure at 2 months of age. Loss of BMPR1A was associated with enhanced proliferation but loss of self-renewal in suture stem cells. Cells from patients were also assessed. Results demonstrate how BMPR1A regulates stemness, clonal expansion, and osteogenesis of suture stem cells, contributing to craniofacial bone development.

Science Translational Medicine (ISSN 1946-6242) is published by the American Association for the Advancement of Science. 1200 New York Avenue NW, Washington, DC 20005. The title *Science Translational Medicine* is a registered trademark of AAAS.